ORIGINAL ARTICLE

Cancer Science WILEY

H19 promotes aerobic glycolysis, proliferation, and immune escape of gastric cancer cells through the microRNA-519d-3p/ lactate dehydrogenase A axis

Linqing Sun[1,2] | Juntao Li[2] | Wenying Yan[3] | Zhendong Yao[2] | Ruoqin Wang[2,4,5] |
Xiaojun Zhou[6] | Hongya Wu[1] | Guangbo Zhang[1,4] | Tongguo Shi[1,4,5] (iD) |
Weichang Chen[1,2]

[1]Jiangsu Institute of Clinical Immunology, The First Affiliated Hospital of Soochow University, Suzhou, China

[2]Department of Gastroenterology, The First Affiliated Hospital of Soochow University, Suzhou, China

[3]Center for Systems Biology, Department of Bioinformatics, School of Biology and Basic Medical Sciences, Soochow University, Suzhou, China

[4]Jiangsu Key Laboratory of Clinical Immunology, Soochow University, Suzhou, China

[5]Jiangsu Key Laboratory of Gastrointestinal Tumor Immunology, The First Affiliated Hospital of Soochow University, Suzhou, China

[6]Department of General Surgery, The First Affiliated Hospital of Soochow University, Suzhou, China

Correspondence
Weichang Chen, Jiangsu Institute of Clinical Immunology, The First Affiliated Hospital of Soochow University, Suzhou, China.
Email: weichangchen@126.com

Tongguo Shi, Jiangsu Institute of Clinical Immunology, The First Affiliated Hospital of Soochow University, Suzhou, China.
Email: shitg@suda.edu.cn

Funding information
National Natural Science Foundation of China, Grant/Award Number: 81802843 and 82073156; Suzhou Science & Technology plan project, Grant/Award Number: SYS2019035.

Abstract

Long noncoding RNAs (lncRNAs) have been investigated in multiple human cancers including gastric cancer (GC). Our research aims to explore the role of H19 in aerobic glycolysis, proliferation, and immune escape of GC cells. The expression of H19 in GC samples was analyzed using Gene Expression Profiling Interactive Analysis, Gene Expression Omnibus data, and real-time quantitative PCR analysis. Relative quantification of glucose consumption and lactate production from cell supernatant were applied to assess the aerobic glycolysis of GC cells. Subcellular fractionation, luciferase reporter, and western blot assays certified the binding between genes. Cell Counting Kit-8 and colony formation assays were used to determine GC cell proliferation. Flow cytometry, ELISA, and real-time quantitative PCR assays were applied to analyze the immunosuppressive effect of H19. H19 was highly expressed in samples of patients with GC, and associated with tumor growth in vivo. H19 knockdown suppressed glucose consumption, lactate production, and proliferation of GC cells by regulating the microRNA (miR)-519d-3p/lactate dehydrogenase A (LDHA) axis. Both miR-519d-3p depletion and LDHA overexpression could reverse the H19 knockdown-induced decrease in aerobic glycolysis and proliferation. Moreover, conditioned medium from stable knockdown H19 GC cells modulated the activity of immune cells including γδT cells, Jurkat cells, and tumor-associated macrophages in a miR-519d-3p/LDHA/

lactate axis-dependent manner. The H19/miR-519d-3p/LDHA axis mainly contributed to aerobic glycolysis, proliferation, and immune escape of GC cells.

1 | INTRODUCTION

Gastric cancer ranked fifth in prevalence and third in mortality around the world according to the 2018 Global Cancer Statistics analysis.[1] Although endoscopy, surgery, and standard chemotherapy have improved the 5-year survival rate of GC patients, the patients with advanced stages and metastasis had an unfavorable prognosis.[2] Consequently, it is worth seeking out new therapeutic targets and clarifying the pathogenesis of GC.

Long noncoding RNA is a type of RNA more than 200 nt in length without protein-coding function.[3] As shown in recent studies, lncRNAs were implicated in multiple human cancers and involved in diverse biological processes of cancers, such as growth, metastasis, drug resistance, metabolism, and immune escape.[4-7] Among the lncRNAs associated with tumor progression, H19 is one of the most well-characterized lncRNAs. A large and growing body of work has shown that *H19* was overexpressed and served as an oncogene in diverse tumors, including breast cancer, colorectal cancer, pancreatic cancer, and GC.[8-12] Zhang et al noted that H19 was overexpressed in GC tissues compared with adjacent normal tissues, and was positively correlated with poor overall survival time.[13] Furthermore, studies have revealed that H19 exerts crucial roles in the regulation of GC cell proliferation, migration, and invasion.[14,15] However, many undefined molecular mechanisms by which H19 contributes to the progression of GC need to be thoroughly investigated.

As a distinctive hallmark of cancer, the Warburg effect or aerobic glycolysis confers on cancer cells a growth advantage by providing energy and biosynthesis building blocks even in the presence of abundant oxygen.[16] Aerobic glycolysis is now widely accepted and serves as an antitumor therapeutic target,[17] but the molecular mechanisms controlling aerobic glycolysis have not been elucidated. Accumulating evidence has indicated that lncRNAs can regulate glucose metabolism in cancer cells by directly regulating the glycolytic enzymes and glucose transporters, or indirectly modulating signaling pathways.[18] For instance, lncRNA AGPG enhanced glycolysis activity and cell proliferation in esophageal squamous cell carcinoma by stabilizing PFKFB3.[19] Zhao and coworkers noted that lncRNA MACC1-AS1 promoted GC cell metabolic plasticity through AMPK/Lin28-mediated mRNA stability of MACC1.[20] Although increased H19 was involved in glycolysis and stemness maintenance in breast cancer stem cells through the let-7/HIF-1α/PDK1 pathway signaling cascade,[21] the effect of H19 on aerobic glycolysis in GC remains largely unknown.

Mounting evidence suggested that aerobic glycolysis in cancer cells has the ability to regulate the immune response in the tumor microenvironment.[22,23] Lactate, a kind of glycolytic metabolite, has been identified as a crucial component that contributes to the immunosuppressive tumor microenvironment.[24] Brand et al showed that tumor-secreted lactate could dampen IFN-γ production by CD8+ T and NK cells and inhibiting their cytolytic activity.[25] Nonetheless, the link connecting H19, aerobic glycolysis, and immune escape in GC cells is still not fully characterized.

In this study, we investigated whether and how H19 modulated aerobic glycolysis, cell proliferation, and immune evasion. Our results showed that the levels of H19 were significantly increased in GC tissue specimens and were associated with a poor prognosis. We further showed that H19 knockdown suppressed aerobic glycolysis and cell proliferation through the miR-519d-3p/LDHA axis in GC cells. Moreover, H19 knockdown modified the activity of γδT cells, T cells, and TAMs, which participate in tumor immune response, in a miR-519d-3p/LDHA/lactate axis-dependent manner.

2 | MATERIALS AND METHODS

### 2.1 | Clinical tissue specimens

Twelve paired fresh tumor tissue specimens and adjacent normal tissue specimens were obtained from patients with GC at the First Affiliated Hospital of Soochow University (Suzhou, China) between May 2017 and August 2018. All tissue specimens were snap-frozen in liquid nitrogen. This study was approved by the Institutional Review Board of the First Affiliated Hospital of Soochow University. Written informed consent was obtained from each patient. Basic clinicopathological information is provided in Table S1.

2.2 | Cell culture

Human GC lines AGS, SGC-7901, and MKN-45, normal gastric mucosa cell GES-1, Jurkat, and THP-1 cells were purchased from the Chinese Academy of Sciences Cell Bank. All cells were cultured in RPMI-1640 (Biological Industries) supplemented with 10% FBS (Biological Industries) and 1% penicillin-streptomycin (Beyotime, #C0222) in a humidified incubator with 5% CO_2 at 37°C.
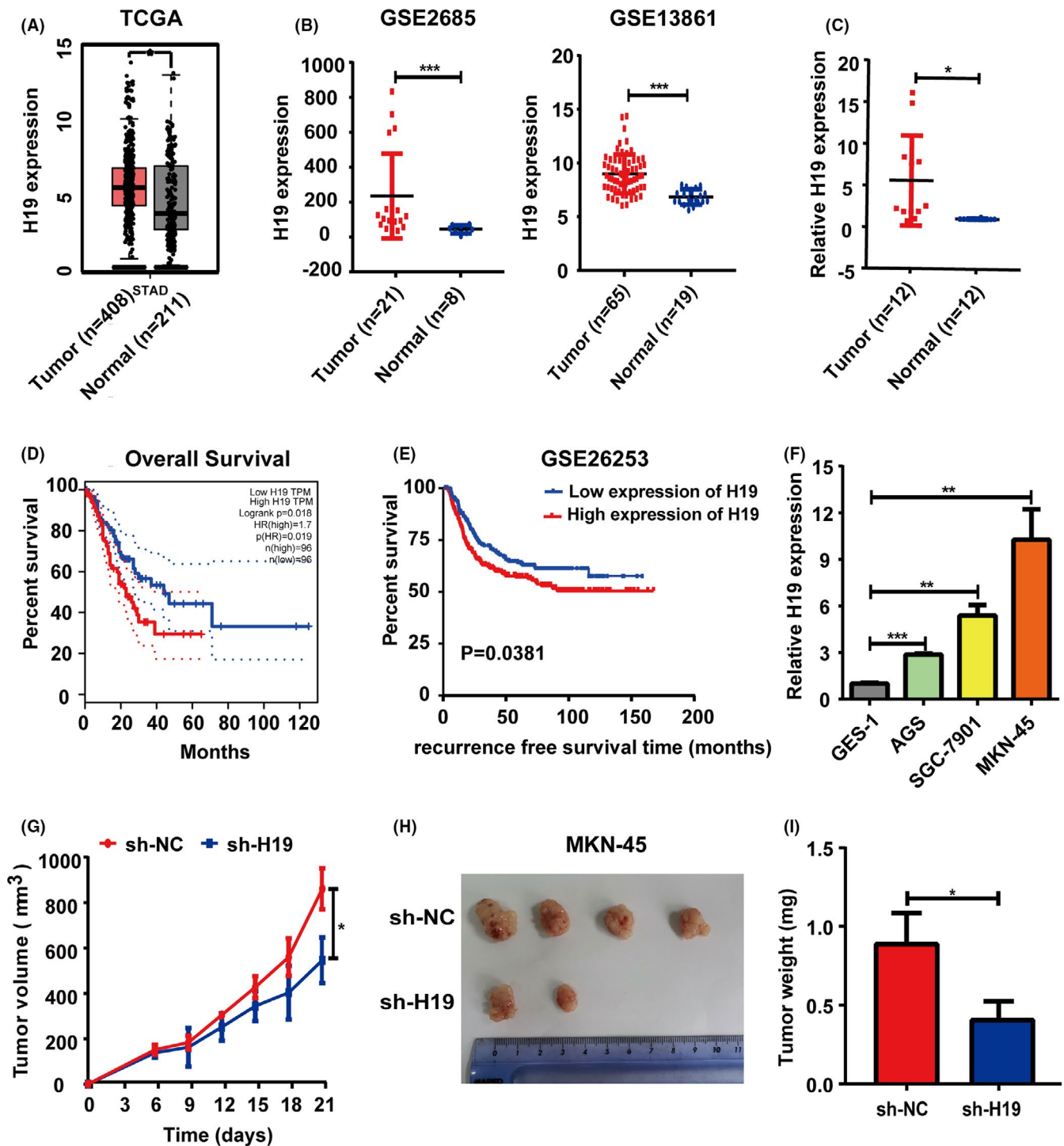
FIGURE 1 H19 was overexpressed in gastric cancer (GC) tissue specimens and promoted tumor growth in vivo. A, Expression of H19 in GC tissue samples from The Cancer Genome Atlas (TCGA) data based on Gene Expression Profiling Interactive Analysis (GEPIA). B, Expression of H19 from GSE2685 and GSE13861 datasets. C, Expression of H19 in 12 pairs of GC and adjacent normal tissue specimens. D, Relationship between the expression of H19 and the overall survival of GC patients from TCGA data based on GEPIA. E, Relationship between the expression of H19 and recurrence-free survival of GC patients from the GSE26253 database. F, Expression of H19 in GES-1, AGS, SGC-7901, and MKN-45 cells. G-I, Tumor volume (G), image (H), and weight (I) of H19 knockdown MKN-45 tumors in nude mice. n = 4 mice per group. Each experiment was carried out in triplicate. Data are presented as the mean ± SD and analyzed by Student's *t*-test. *P < .05, **P < .01, ***P < .001. HR, hazard ratio; sh-NC, negative control; TPM, transcripts per million
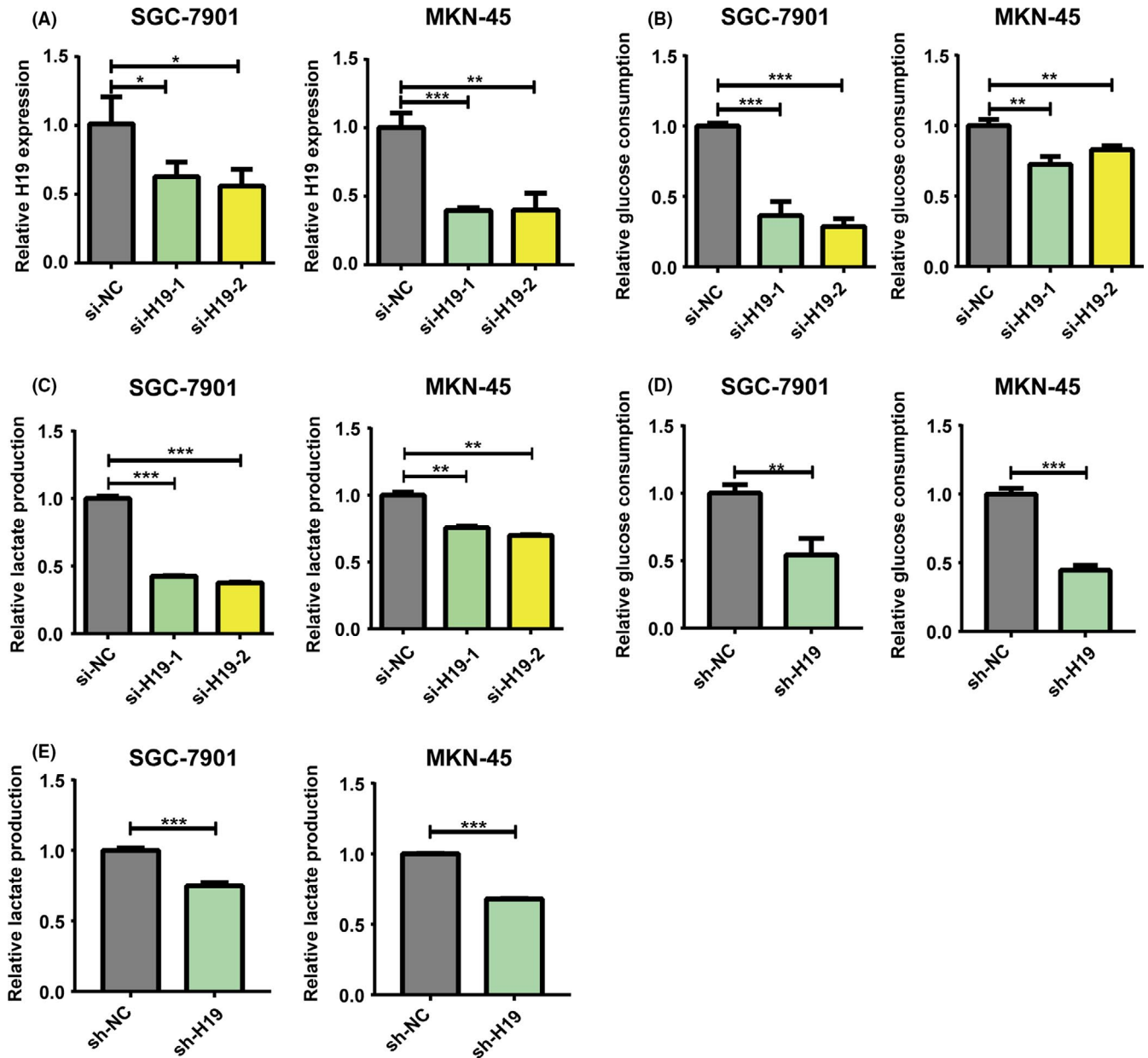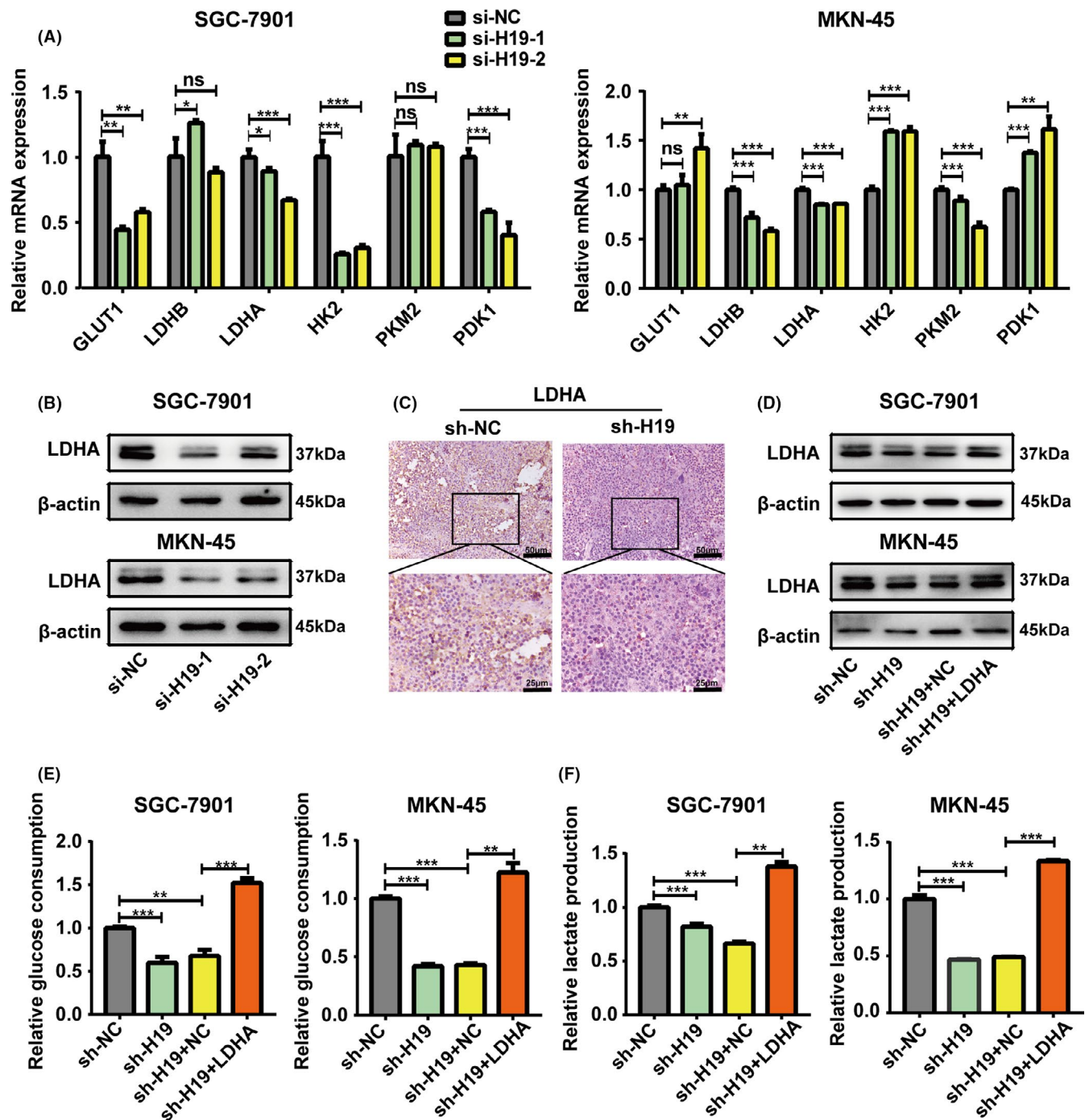
FIGURE 2 H19 knockdown inhibited aerobic glycolysis in gastric cancer cells. A, H19 levels in SGC-7901 and MKN-45 cells were analyzed by real-time quantitative PCR after transfection with siRNA negative control (si-NC), H19 siRNA-1 (si-H19-1), or H19 siRNA-2 (si-H19-2). B, C, Glucose consumption (B) and lactate production (C) were measured in SGC-7901 and MKN-45 cells after transfection with si-NC, si-H19-1, or si-H19-2. D, E, Glucose consumption (D) and lactate production (E) were measured in both stable knockdown H19 (sh-H19) SGC-7901 and MKN-45 cells. Each experiment was carried out in triplicate. Data are presented as the mean ± SD and analyzed by Student's t-test. *P < .05, **P < .01, ***P < .001

2.3 | RNA isolation and RT-qPCR

Total RNA from tissue samples or cells was extracted using TRIzol reagent (TaKaRa) according to the manufacturer's instructions. For gene expression analysis, a total of 1 μg RNA was reverse-transcribed into cDNA using PrimeScript RT Master Mix (Takara, #RR036A). The RT-qPCR reactions were undertaken on a CFX96 Touch real-time PCR system (Bio-Rad) using AceQ universal SYBR qPCR Master Mix (Vazyme, #Q511) according to the manufacturer's instructions. For miRNA expression analysis, 1 μg total RNA was used for first-strand DNA synthesis using a miRNA 1st Strand cDNA Synthesis Kit (Vazyme, #MR101-02), and RT-qPCR was carried out using a miRNA universal SYBR qPCR Master Mix kit (Vazyme, #MQ101-02). Sample and reference genes were analyzed in triplicate. Individual gene expression was normalized to β-actin, and miRNA expression was normalized to small nuclear RNA U6. The primer sequences for RT-qPCR are provided in Table S2.

FIGURE 3 H19 knockdown inhibited aerobic glycolysis through lactate dehydrogenase A (LDHA). A, The expression of glycolysis-related genes was examined by real-time quantitative PCR in SGC-7901 and MKN-45 cells after transfection with siRNA negative control (si-NC), H19 siRNA-1 (si-H19-1), or H19 siRNA-2 (si-H19-2). B, LDHA protein level was detected by western blot in SGC-7901 and MKN-45 cells after transfection with si-NC, si-H19-1, or si-H19-2. β-Actin served as a loading control. C, LDHA immunohistochemical staining in xenograft tumor tissues from the sh-H19 or sh-NC group. One representative image is shown. D, LDHA protein level was detected by western blot in both sh-H19 SGC-7901 and MKN-45 cells after transfection with negative control plasmid (NC) or LDHA overexpression plasmid (LDHA). β-Actin served as a loading control. E, F, Glucose consumption (E) and lactate production (F) were examined in sh-H19 SGC-7901 and MKN-45 cells after transfection with NC or LDHA. Each experiment was carried out in triplicate. Data are presented as the mean ± SD and analyzed by Student's t-test. *P < .05, **P < .01, ***P < .001. GLUT1, glucose transporter type 1; HK2, hexokinase 2; LDHB, lactate dehydrogenase B; ns, not significant; PDK1, phosphoinositide-dependent kinase-1; PKM2, pyruvate kinase M2

2.4 | Conditioned medium

Cells (3×10^5) were seeded in 6-well plates and cultured overnight. The culture medium was changed to fresh medium in each well. After 24 hours, the CM was collected.

2.5 | γδT cell separation and culture

γδT cells were isolated from human PBMCs and cultured as previously described.[26]

2.6 | Other methods

Detailed descriptions of other methods used in this study are provided in Appendix S1.

2.7 | Statistical analysis

All data were presented as mean ± SD. Student's t-test was used for comparisons between two groups. For survival curves, the Kaplan-Meier method with log-rank or Gehan-Breslow-Wilcoxon test was used. Significant differences were displayed as follows: *$P < .05$, **$P < .01$, and ***$P < .001$.

3 | RESULTS

3.1 | H19 was overexpressed in GC tissue specimens and promoted tumor growth in nude mice

Based on a new database visualization website of GEPIA with TCGA data (http://gepia.cancer-pku.cn/), the expression of H19 was significantly increased in GC tissue samples compared with normal samples (Figure 1A). GSE2685 and GSE13861 microarray data from Gene Expression Omnibus databases (http://www.ncbi.nlm.nih.gov/gds/) also showed that the H19 levels were upregulated in GC tissue samples (Figure 1B). To corroborate the above results, we investigated the H19 expression levels in 12 pairs of fresh GC tissues and corresponding normal adjacent tissues by RT-qPCR assay,
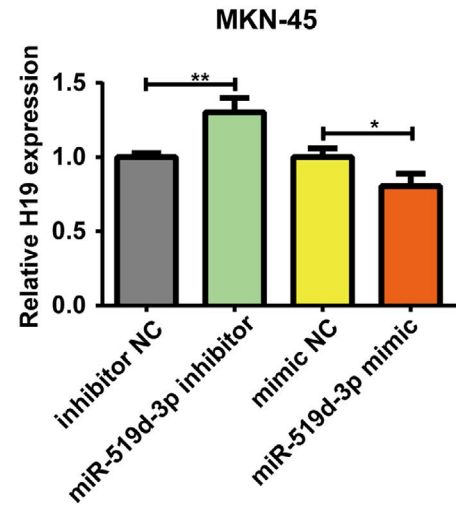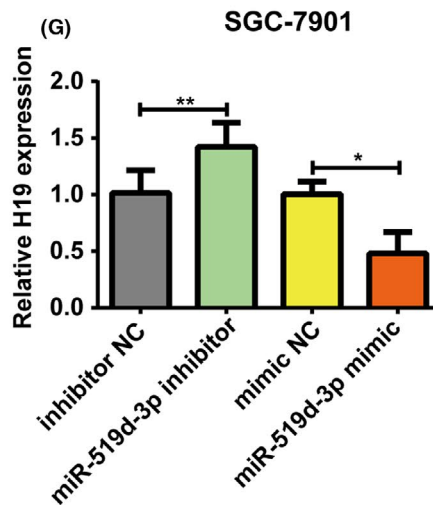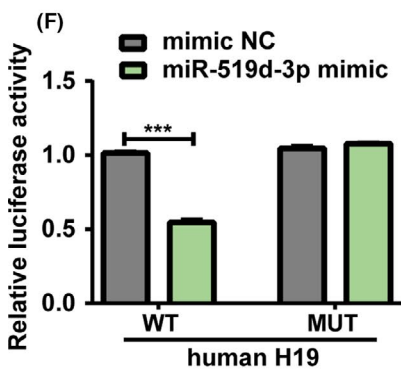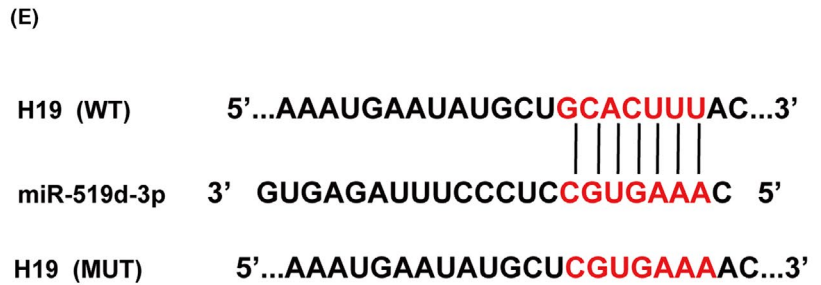
and found that the relative expression of H19 was higher in tumor tissues than that in normal tissues (Figure 1C). We further evaluated the prognostic value of H19 in GC using GEPIA with TCGA data and GSE26253 microarray data. As shown in Figure 1D, GC patients with high H19 expression had a shorter overall survival in TCGA data. Moreover, high expression of H19 predicted shorter recurrence-free sur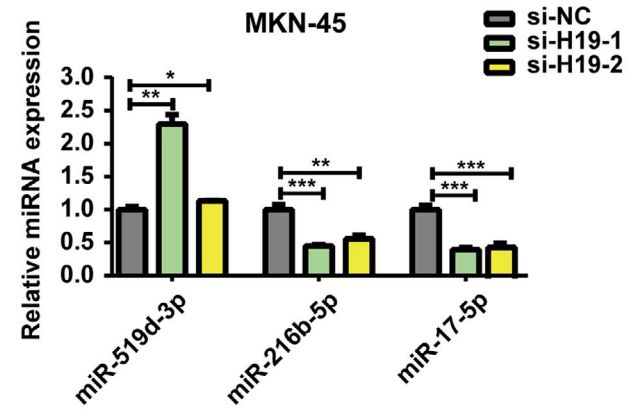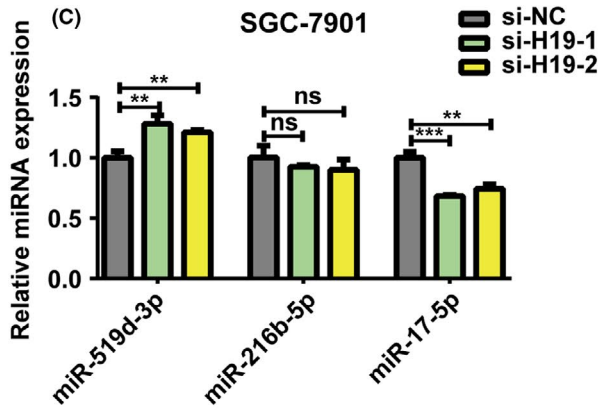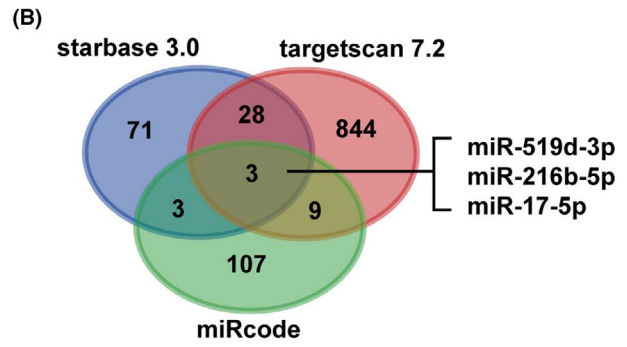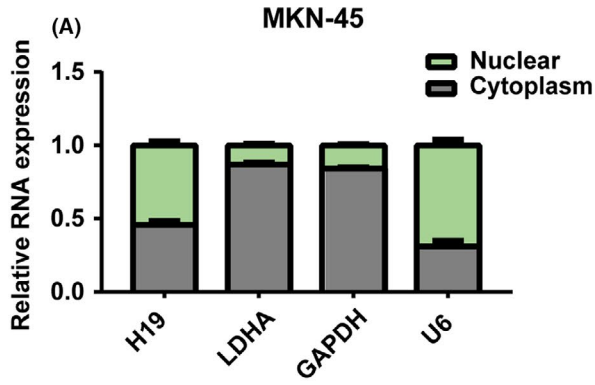vival in GSE26253 microarray data (Figure 1E). Next, the expression levels of H19 in normal gastric mucosa cell GES-1 and three GC cell lines AGS, MKN-45, and SGC-7901 cells were examined. The RT-qPCR results noted that H19 was overexpressed in GC cell lines (Figure 1F).

We further used two nonoverlapping siRNAs targeting H19 (si-H19-1 and si-H19-2) to knock down the expression of H19 in GC cells (Figure 2A). The sequences of si-H19-2 were chosen to construct the shRNA lentivirus (sh-H19), which mediated stably downregulating H19 expression in MKN-45 and SGC-7901 cells (Figure S1A-D). To investigate the effect of H19 on tumor growth in vivo, we established a nude mouse xenograft tumor model using stable knockdown H19 MKN-45 cells (Figure 1G-I). The tumor sizes, images, and mass revealed that H19 knockdown significantly suppressed MKN-45 tumor growth (Figure 1G-I). Collectively, these data showed that H19 was highly expressed in a subset of patients with GC, and was positively associated with tumor growth in vivo.

3.2 | H19 knockdown inhibited glucose consumption and lactate production in GC cells

Given that H19 could regulate aerobic glycolysis in breast cancer stem cells and ovarian cancer cells,[21,27] we hypothesized that H19 might be involved in the glycolysis process in GC cells. Hence, the H19 knockdown cell model was established by transfecting SGC-7901 and MKN-45 cells with two siRNAs (si-H19-1 and si-H19-2) (Figure 2A). As shown in Figure 2B, H19 depletion dramatically reduced the glucose consumption in SGC-7901 and MKN-45 cells. Moreover, we also analyzed the effect of H19 suppression on lactate production and found that the silencing of H19 significantly inhibited lactate production (Figure 2C). Consistent with the above results, the glucose consumption and lactate production were also clearly decreased in stable knockdown H19 SGC-7901 or MKN-45 cells (Figure 2D,E). These results indicated that H19 knockdown inhibited aerobic glycolysis in GC cells.

FIGURE 4 H19 sponged microRNA (miR)-519d-3p in gastric cancer cells. A, Subcellular distribution of H19 and lactate dehydrogenase A (LDHA) was examined by nuclear and cytoplasmic separation experiments with real-time quantitative PCR (RT-qPCR) in MKN-45 cells. B, Three putative miRNAs targeting both H19 and LDHA were predicted by three different algorithms (starBase 3.0 for H19, TargetScan 7.2 for LDHA, and miRcode for H19). C, Levels of miR-519d-3p, miR-216b-5p, and miR-17-5p were detected by RT-qPCR in SGC-7901 and MKN-45 cells after transfection with siRNA negative control (si-NC), H19 siRNA-1 (si-H19-1), or H19 siRNA-2 (si-H19-2). D, Levels of miR-519d-3p in the xenograft tumor tissues from the sh-H19 or sh-NC group were measured by RT-qPCR. E, Hybridization models between H19 and miR-519d-3p. F, Luciferase reporter assay showed the binding of miR-519d-3p and WT H19 but not mutant (MUT) H19. G, mRNA levels of H19 were measured by RT-qPCR in both SGC-7901 and MKN-45 cells after transfection with inhibitor negative control (NC), miR-519d-3p inhibitor, mimic NC, or miR-519d-3p mimic. Each experiment was carried out in triplicate. Data are presented as the mean ± SD and analyzed by Student's t-test. *$P < .05$, **$P < .01$, ***$P < .001$. ns, not significant

(A) MKN-45

(B) starbase 3.0 / targetscan 7.2 / miRcode
miR-519d-3p
miR-216b-5p
miR-17-5p

(C) SGC-7901 / MKN-45

(D)

(E)
H19 (WT) 5'...AAAUGAAUAUGCUGCACUUUAC...3'
miR-519d-3p 3' GUGAGAUUUCCCUCCGUGAAAC 5'
H19 (MUT) 5'...AAAUGAAUAUGCUCGUGAAAAC...3'

(F) human H19
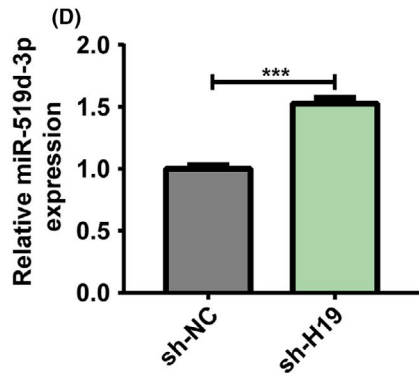
(G) SGC-7901 / MKN-45

3.3 | H19 regulated aerobic glycolysis via LDHA

To elucidate the mechanisms that H19 knockdown suppressed aerobic glycolysis, a spectrum of key glycolysis-related genes was examined in H19 knockdown SGC-7901 and MKN-45 cells by RT-qPCR. The results showed that compared with glucose transporter type 1, LDHB, hexokinase 2, PKM2, and PDK1, the mRNA expression level of LDHA was positively correlated with the expression level of H19 in SGC-7901 and MKN-45 cells (Figure 3A). Moreover, H19 knockdown reduced the protein expression of LDHA in SGC-7901 and MKN-45 cells (Figures 3B and S2A). Importantly, the immunohistochemistry and RT-qPCR assays revealed that the protein and mRNA expression of LDHA was much lower in the xenograft tissues from the sh-H19 group than in the sh-NC group (Figures 3C and S2B).

To explore whether LDHA contributed to H19-mediated glycolysis, we obtained a commercial LDHA overexpression plasmid (LDHA), which markedly upregulated the LDHA protein level in SGC-7901 and MKN-45 cells (Figure S2C). As shown in Figure 3D, transfection with LDHA overexpression plasmid abolished the effect of H19 suppression on the protein expression of LDHA in SGC-7901 and MKN-45 cells (Figures 3D and S2D). More importantly, LDHA overexpression reversed the H19 depletion-induced decrease in glucose consumption and lactate production (Figure 3E,F). In addition, we found that transfection with si-H19-1 significantly inhibited glucose consumption and lactate production, whereas cotransfection of si-H19-1 and LDHA overexpression plasmid could cancel out this effect in SGC-7901 and MKN-45 cells (Figure S3).

3.4 | H19 regulated LDHA expression and glycolysis in a miR-519d-3p-dependent manner

To explore how H19 regulated LDHA expression in GC cells, we carried out cytoplasmic and nuclear separation experiments with RT-qPCR to determine the subcellular localization of H19 and LDHA. The results showed that H19 was distributed in both the nucleus and cytoplasm, whereas LDHA was predominantly localized in the cytoplasm (Figure 4A). Moreover, the predicted results of lncATLAS (http://lncatlas.crg.eu/) also indicated that H19 was localized in both the nucleus and cytoplasm (Figure S4). Therefore, we speculated that H19 might function as a ceRNA to regulate LDHA expression by sponging one or several specific miRNAs. Hence, we predicted the possible binding miRNAs of H19 and LDHA by using three publicly available prediction tools starBase 3.0 (for H19), TargetScan 7.2 (for LDHA), and miRcode (for H19). As shown in Figure 4B, three miRNAs (miR-519d-3p, miR-216b-5p, and miR-17-5p) could bind to both H19 and LDHA. Subsequently, the levels of the three candidate miRNAs were detected by RT-qPCR, and the results revealed that miR-519d-3p expression was significantly increased in H19 knockdown SGC-7901 and MKN-45 cells (Figure 4C). In addition, the expression of miR-519d-3p was markedly upregulated in the xenograft tissues from the sh-H19 group compared with the sh-NC group (Figure 4D). As shown in Figure 4E, we showed the hybridization models between H19 and miR-519d-3p. Next, we undertook luciferase reporter assays to determine whether miR-519d-3p could directly regulate H19. Overexpression of miR-519d-3p impaired the luciferase activity of the pmirGLO-H19-WT vector but failed to reduce that of the pmirGLO-H19-MUT vector (Figure 4F). Moreover, the results of RT-qPCR also indicated that the downregulation of miR-519d-3p significantly increased the levels of H19 in SGC-7901 and MKN-45 cells, whereas miR-519d-3p overexpression reduced the levels of H19 (Figure 4G).
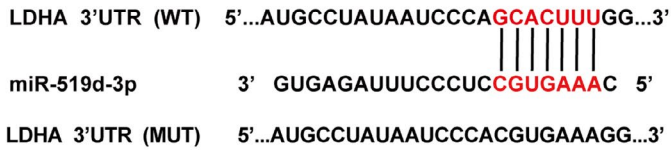
The hybridization models between LDHA and miR-519d-3p are shown in Figure 5A. Luciferase reporter assays confirmed the direct interaction between LDHA and miR-519d-3p. The miR-519d-3p mimic reduced the luciferase activity of the pmirGLO-LDHA-WT vector but failed to decrease that of the pmirGLO-LDHA-MUT vector (Figure 5B). MicroRNA-519d-3p knockdown elevated, whereas miR-519d-3p overexpression reduced, the mRNA and protein expression of LDHA in SGC-7901 and MKN-45 cells (Figures 5C,D and S5A).

We also undertook the rescue experiments. The results indicated that downregulation of miR-519d-3p could counteract the increases in miR-519d-3p expression induced by H19 knockdown in SGC-7901 and MKN-45 cells (Figure S5B). Additionally, miR-519d-3p inhibitor reversed the decreases in LDHA mRNA and protein expression in stable knockdown H19 SGC-7901 and MKN-45 cells (Figures 5E,F and S5C). Furthermore, miR-519d-3p knockdown abolished the effect of H19 suppression on glucose consumption and lactate production in SGC-7901 and MKN-45 cells (Figure 5G,H). Additionally, H19 knockdown could inhibit glucose consumption and lactate production, whereas cotransfection of si-H19-1 and miR-519d-3p inhibitor had no effect on glucose consumption and lactate production in SGC-7901 and MKN-45 cells (Figure S6). These data suggested that H19 could modulate LDHA expression and glycolysis by sponging miR-519d-3p.
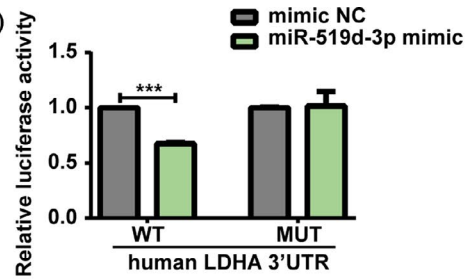
FIGURE 5 H19 regulated lactate dehydrogenase A (LDHA) expression and glycolysis through microRNA (miR)-519d-3p. A, Hybridization models between LDHA and miR-519d-3p. B, Luciferase reporter assay showed the binding of miR-519d-3p and WT LDHA 3′-UTR but not mutant (MUT) LDHA 3′-UTR. C, D, mRNA (C) and protein (D) levels of LDHA were measured in both SGC-7901 and MKN-45 cells after transfection with inhibitor negative control (NC), miR-519d-3p inhibitor, mimic NC, or miR-519d-3p mimic. β-Actin served as a loading control. E, F, mRNA (E) and protein (F) levels of LDHA were measured in both sh-H19 SGC-7901 and MKN-45 cells after transfection with inhibitor NC or miR-519d-3p inhibitor. β-Actin served as a loading control. G, H, Glucose consumption (G) and lactate production (H) were examined in both sh-H19 SGC-7901 and MKN-45 cells after transfection with inhibitor NC or miR-519d-3p inhibitor. Each experiment was carried out in triplicate. Data are presented as the mean ± SD and analyzed by Student's *t*-test. *$P < .05$, **$P < .01$, ***$P < .001$
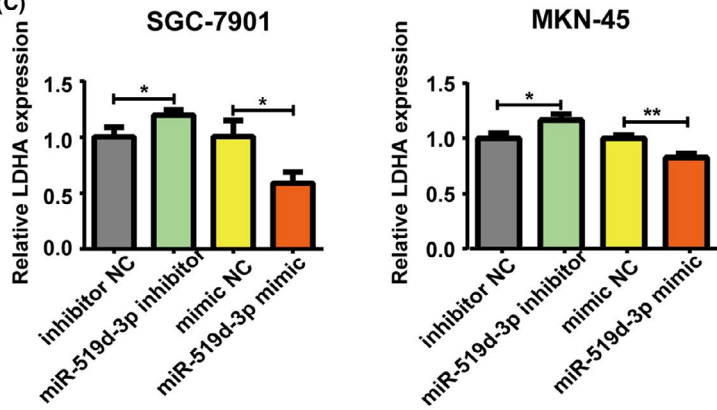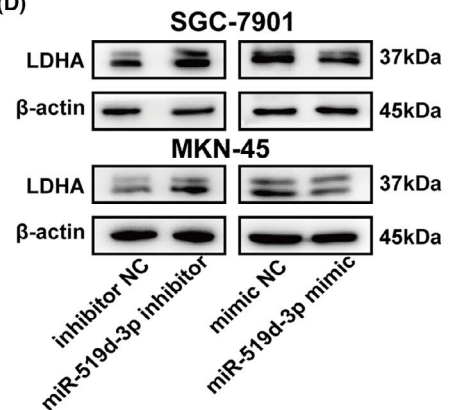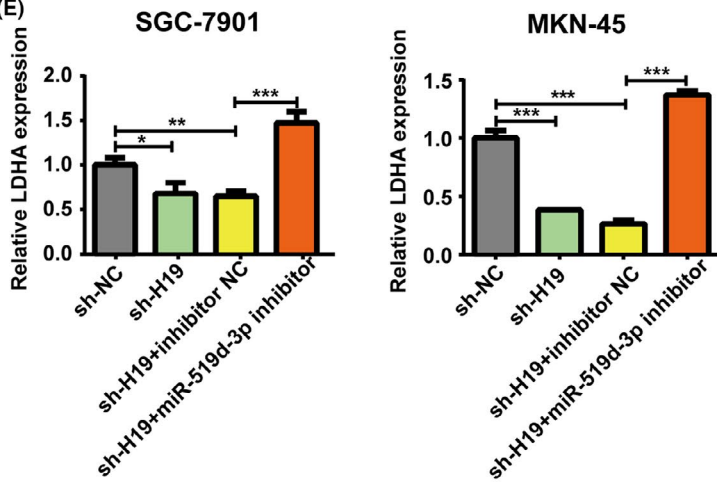
(A)

LDHA 3'UTR (WT)   5'...AUGCCUAUAAUCCCAGCACUUUGG...3'

miR-519d-3p   3' GUGAGAUUUCCCUCCGUGAAAC 5'

LDHA 3'UTR (MUT)   5'...AUGCCUAUAAUCCCACGUGAAAGG...3'
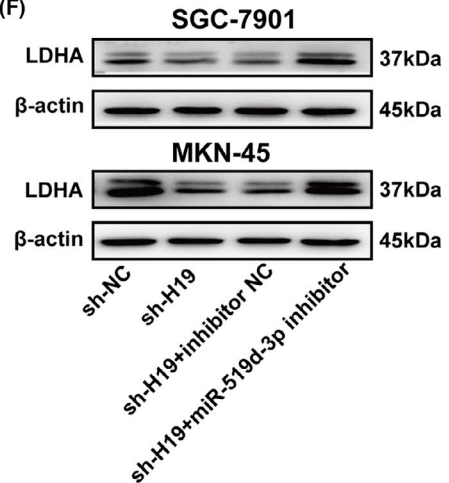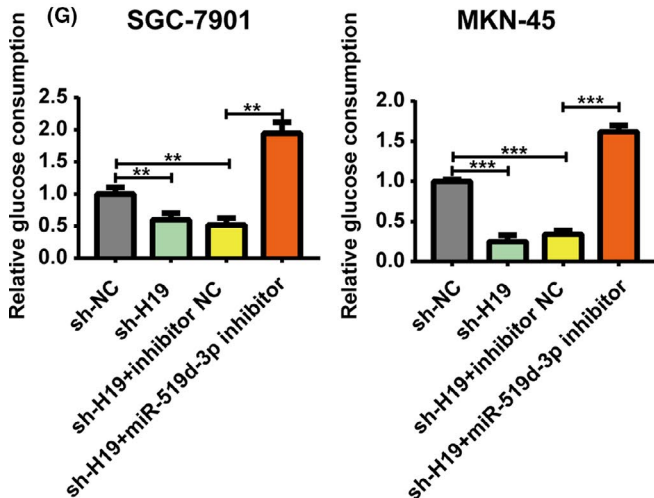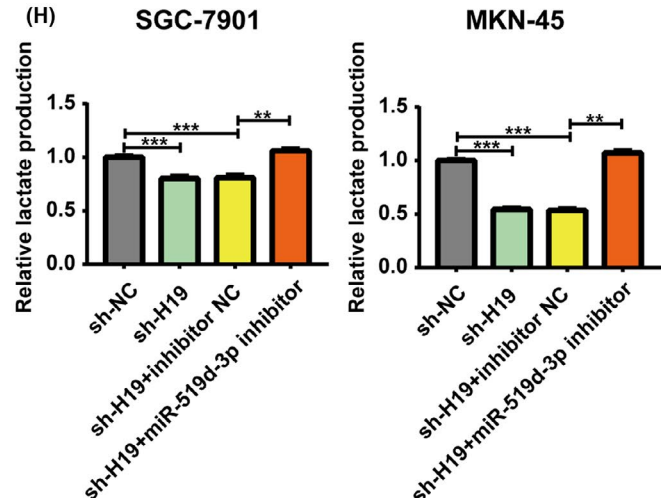
3.5 | H19 knockdown suppressed GC cell proliferation through the miR-519d-3p/LDHA axis

Notably, H19 has been reported to promote cancer cell proliferation through multiple mechanisms.[28-30] Herein, we investigated the effect of H19 knockdown on GC cell proliferation and explored the underlying molecular mechanisms. The CCK-8 assay indicated that H19 knockdown significantly decreased the proliferation rate of GC cells (Figure 6A,B). These results were further confirmed by clonogenic assay (Figure 6C,D). Given that H19 modulated glycolysis through regulating LDHA expression in a miR-519d-3p-dependent manner, we next determined whether H19 was involved in GC cell growth through the miR-519d-3p/LDHA axis. Rescue experiments validated that the effect of H19 knockdown on GC cell proliferation rate and colony formation was reversed by miR-519d-3p depletion and LDHA overexpression (Figure 6).

3.6 | H19 modulated immune escape through the miR-519d-3p/LDHA/lactate axis

Previous studies have shown that lactate, a major glycolytic metabolite, could modify tumor immune response.[25,31] Also, our results indicated that H19 knockdown markedly decreased the accumulation of extracellular levels of lactate (Figure 2C,E). Therefore, we asked whether H19 was able to modulate tumor immune response through the miR-519d-3p/LDHA/lactate axis. As shown in Figure 7A, CM from stable knockdown H19 GC cells clearly elevated the population of IFN-γ-positive (IFN-γ^{+}) γδT cells, an important antitumor immune cell.[32] Moreover, treatment with lactate counteracted the increases in the population of IFN-γ^{+} γδT cells induced by CM from stable knockdown H19 GC cells (Figure 7A). Conditioned medium from stable knockdown H19 GC cells treated with miR-519d-3p inhibitor or LDHA overexpression plasmid had similar results (Figure 7A). Furthermore, the addition of lactate or treatment with CM from stable knockdown H19 GC cells transfected with miR-519d-3p inhibitor or LDHA overexpression plasmid also reduced the IL-2 expression in PMA and ionomycin-activated Jurkat cells, which was enhanced by CM from stable knockdown H19 GC cells (Figure 7B).

We also investigated whether H19 signaling could modulate TAM generation from human monocyte cell line THP-1. After treatment with PMA for 24 hours, THP-1 cells were cultured with CM from stable knockdown H19 GC cells. The results of RT-qPCR showed that macrophages treated with CM from stable knockdown H19 GC cells showed higher levels of M1 markers nitric oxide synthase 2, C-X-C motif chemokine ligand 9, tumor necrosis factor-α, and HLA-DR, but
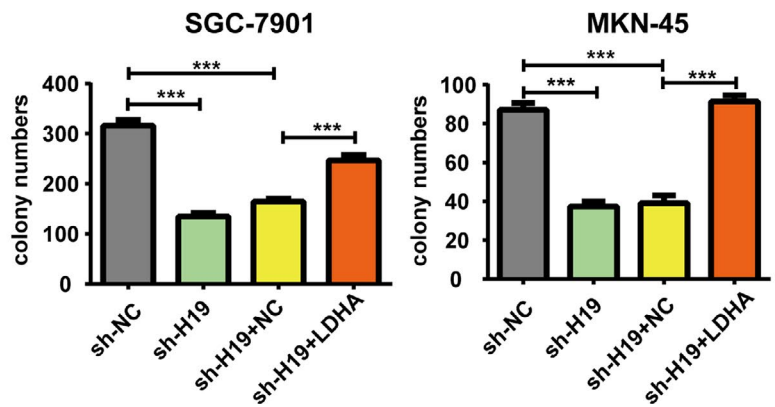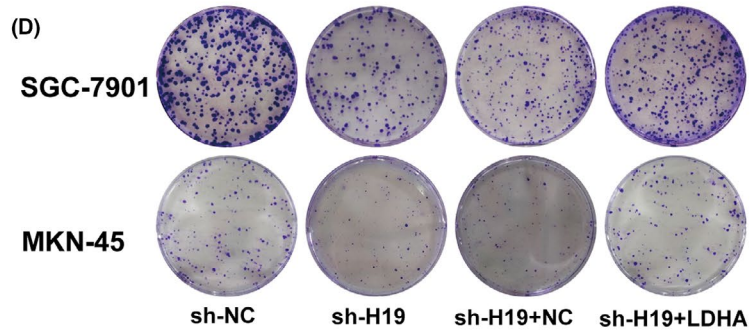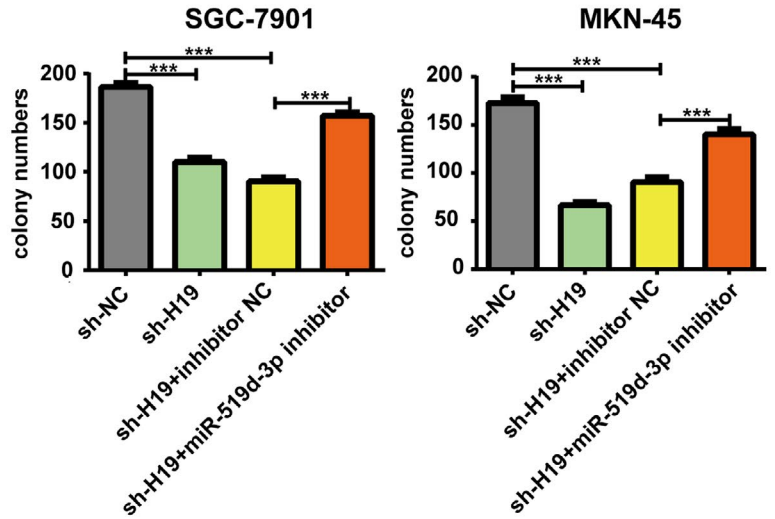
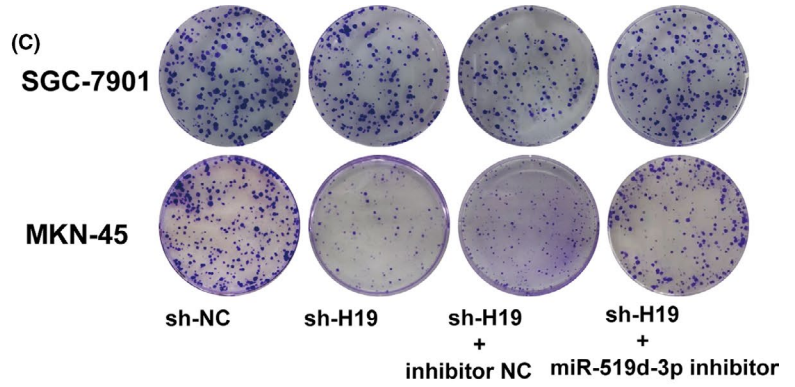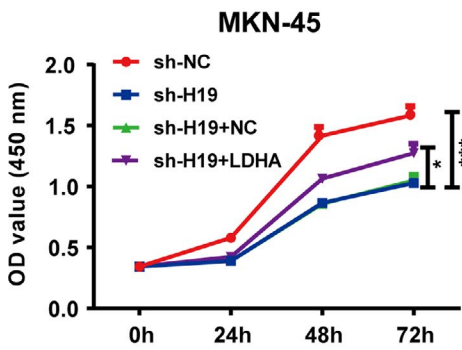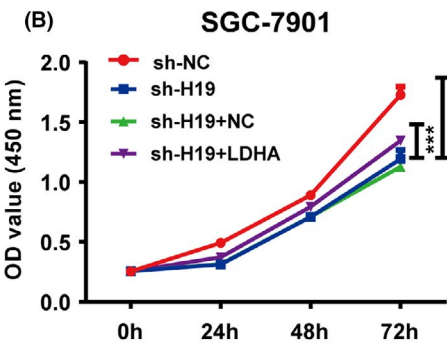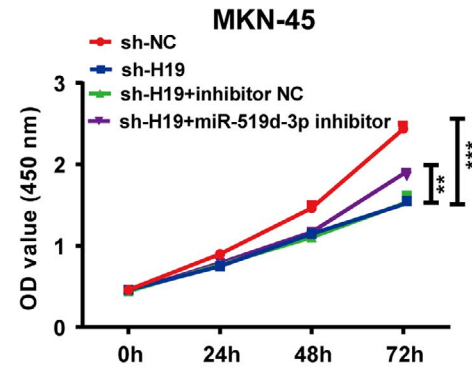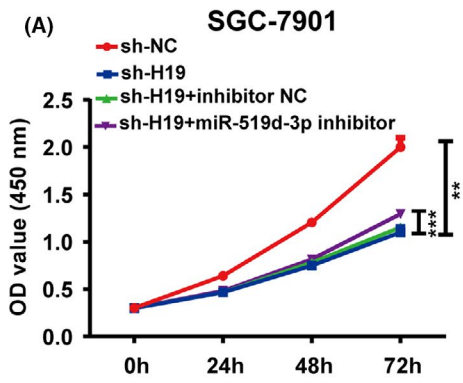lower levels of M2 markers arginase 1 and transforming growth factor-β (Figure 7C). Treatment with lactate or CM from stable knockdown H19 GC cells transfected with miR-519d-3p inhibitor or LDHA overexpression plasmid abolished the effect of CM from stable knockdown H19 GC cells on TAM generation (Figure 7C). In addition, the population of CD163^{+} TAMs was significantly decreased in nos2xenograft tissues from the sh-H19 group compared with the sh-NC group (Figure S7). The above results indicated that H19 signaling modulated the activity of immune cells including γδT cells, Jurkat cells, and TAMs, which might contribute to the immune escape of GC cells.
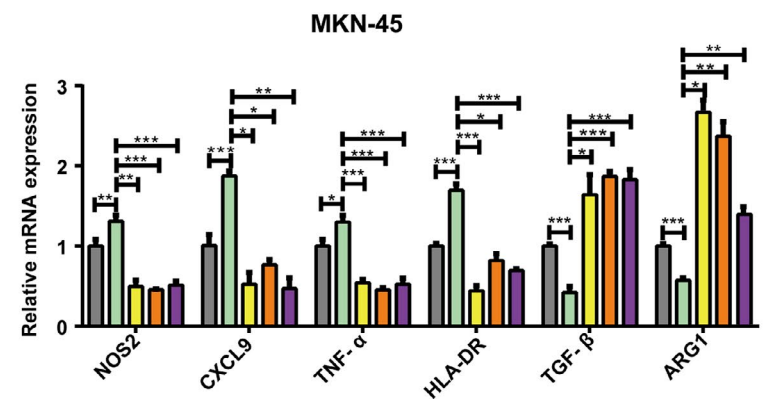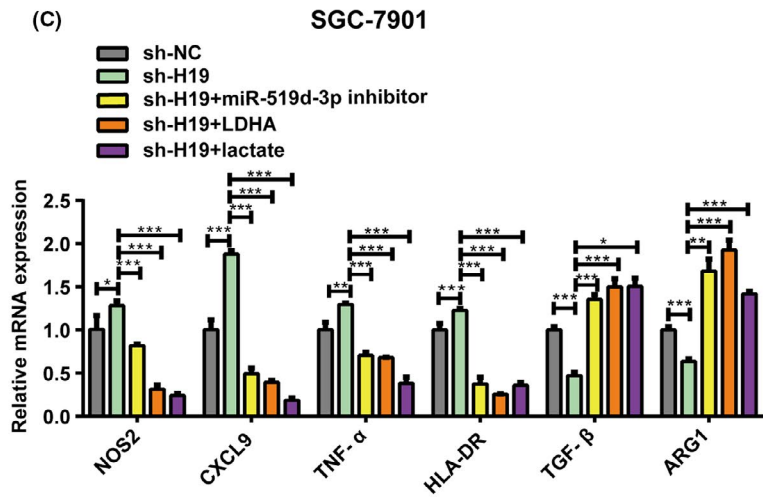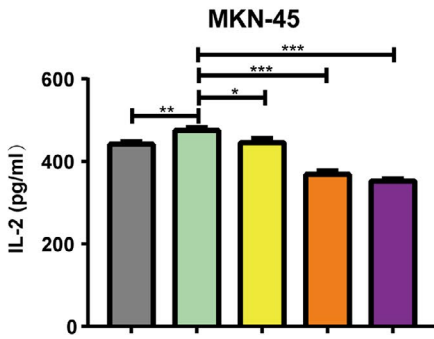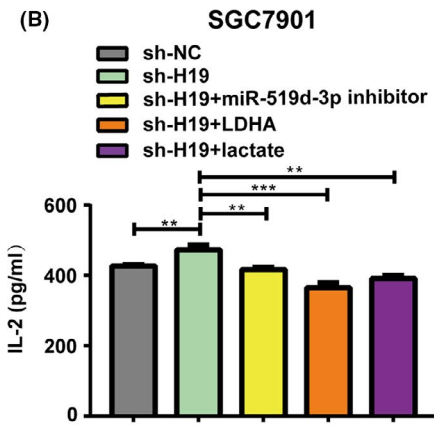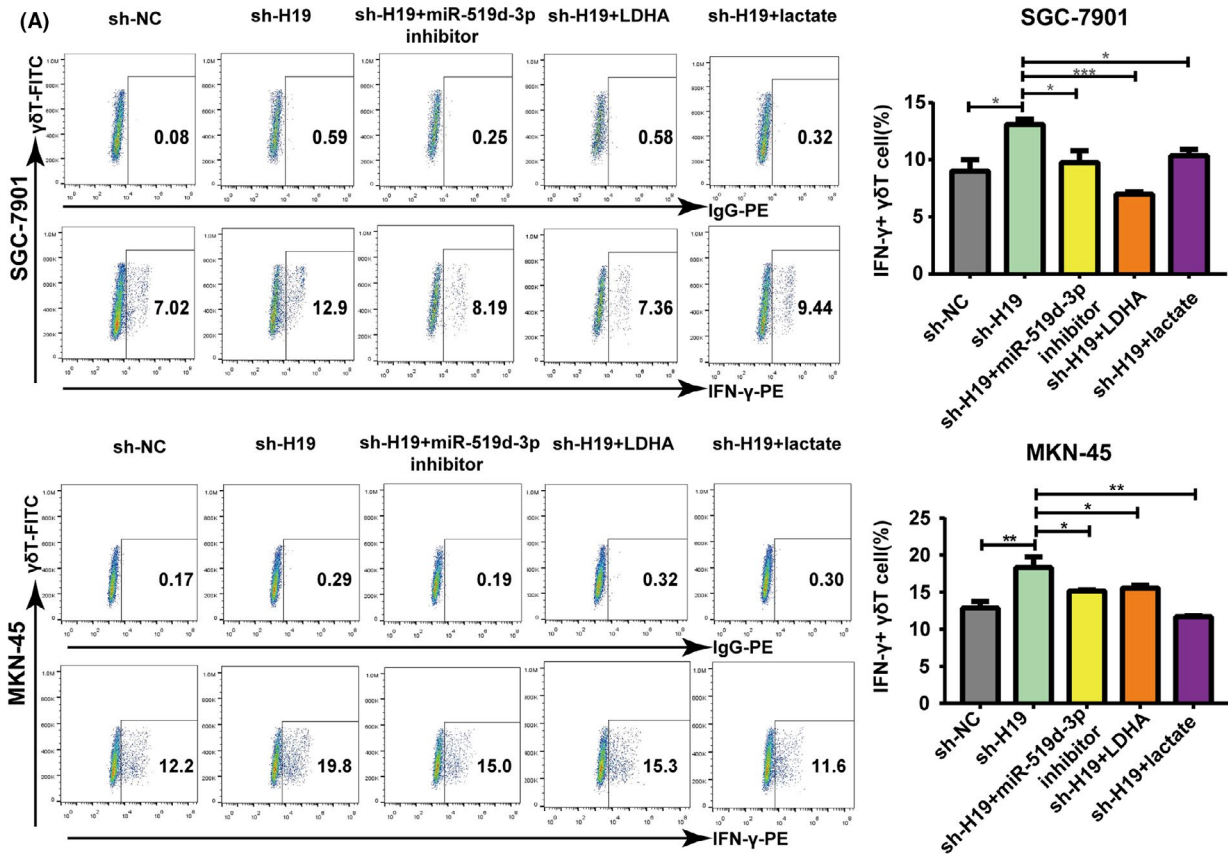
4 | DISCUSSION

H19 has been identified to act as an important regulator in the tumorigenesis and progression of GC. For instance, upregulated H19 was associated with lymph node metastasis and TNM stage of GC patients and promoted cell growth and metastasis through the miR-22-3p/Snail1 signaling pathway in GC.[33] H19-derived miR-675 was reported to enhance the proliferation and invasion of GC cells through RUNX1.[34] Herein, findings from our study were consistent with previous reports that H19 was highly expressed in GC tissues and was associated with the poor prognosis of patients with GC. Using a nude mouse xenograft tumor model, H19 knockdown was found to significantly suppress tumor growth in vivo. More importantly, we found that H19 modulated the aerobic glycolysis, proliferation, and immune escape of GC cells by sponging miR-519d-3p to induce the expression of LDHA (Figure 8).

Previous studies noted that H19 participated in cancer cell aerobic glycolysis. The H19/let-7/HIF-1α signaling-mediated PDK1 could regulate glycolysis, and further contribute to breast cancer stem cell maintenance under hypoxic conditions.[21] In ovarian cancer, H19 overexpression increased glucose consumption, lactate production, and PKM2 expression in SKOV3 and A2780 cells treated with ginsenoside 20(S)-Rg3.[27] The above studies showed the important roles of H19 in the regulation of aerobic glycolysis in cancers, but the effect of H19 on aerobic glycolysis in GC remains largely unknown. In this study, we found that H19 knockdown decreased glucose consumption and lactate production in GC cells. Moreover, the mRNA and protein levels of LDHA were positively associated with H19 levels in GC cells. Importantly, LDHA was highly expressed in GC samples,[35,36] and involved in glucose metabolism, proliferation, and migration of GC cells.[37,38] Therefore, we inferred that H19 participated in GC aerobic glycolysis by regulating LDHA. Our results indicated that LDHA overexpression reversed the H19 depletion-induced decreases in glucose consumption and lactate production

FIGURE 6 H19 knockdown suppressed gastric cancer cell proliferation through the microRNA (miR)-519d-3p/lactate dehydrogenase A (LDHA) axis. A, B, Cell viability of sh-H19 SGC-7901 and MKN-45 cells was analyzed by CCK-8 after transfection with miR-519d-3p inhibitor (A) or LDHA overexpression plasmid (B). C, D, Colony formation assay of sh-H19 SGC-7901 and MKN-45 cells after transfection with miR-519d-3p inhibitor (C) or LDHA overexpression plasmid (D). Each experiment was carried out in triplicate. Data are presented as the mean ± SD and analyzed by Student's t-test. *P < .05, **P < .01, ***P < .001. OD, optical density

(A) SGC-7901 / MKN-45 — sh-NC, sh-H19, sh-H19+inhibitor NC, sh-H19+miR-519d-3p inhibitor

(B) SGC-7901 / MKN-45 — sh-NC, sh-H19, sh-H19+NC, sh-H19+LDHA

(C) SGC-7901 / MKN-45 colony formation and colony numbers

(D) SGC-7901 / MKN-45 colony formation and colony numbers

FIGURE 7 H19 knockdown affected tumor immune response through the microRNA (miR)-519d-3p/ lactate dehydrogenase A (LDHA)/ lactate axis. A, Population of interferon-γ (IFN-γ)⁺ γδT cells among γδT cells treated with conditioned medium (CM) from sh-H19 SGC-7901 and MKN-45 cells (sh-H19), CM from sh-H19 SGC-7901 and MKN-45 cells after transfection with miR-519d-3p inhibitor (sh-H19 + miR-519d-3p inhibitor), or CM from sh-H19 SGC-7901 and MKN-45 cells after transfection with LDHA overexpression plasmid (sh-H19 + LDHA) or lactate. B, Concentrations of interleukin-2 (IL-2) in the supernatants of PMA and ionomycin-activated Jurkat cells treated with sh-H19, sh-H19 + miR-519d-3p inhibitor, sh-H19 + LDHA or lactate. C, Expression of the markers of M1 and M2 macrophages in PMA-treated THP-1 macrophages treated with sh-H19, sh-H19 + miR-519d-3p inhibitor, sh-H19 + LDHA or lactate. Each experiment was carried out in triplicate. Data are presented as the mean ± SD and analyzed by Student's *t*-test. *$P < .05$, **$P < .01$, ***$P < .001$. ARG1, arginase 1; CXCL9, C-X-C motif chemokine ligand 9; NOS2, nitric oxide synthase 2; PE, phycoerythrin; TGF-β, transforming growth factor-β; TNF-α, tumor necrosis factor-α

in SGC-7901 and MKN-45 cells. In breast cancer stem cells, H19 knockdown decreased PDK1 expression through the let-7/HIF-1α axis in hypoxia, and ablation of PDK1 counteracted H19-mediated glycolysis, suggesting that H19 modulated glycolysis through the let-7/HIF-1α/PDK1 axis.[21] In the current study, our data suggested that the important effect of H19 on GC aerobic glycolysis is LDHA-dependent in the presence of a rich oxygen supply. We cannot explain the roles of H19 in modulating aerobic glycolysis in GC cells under hypoxic conditions. Further investigations are required to answer this question.

It is well known that the biological function of lncRNAs is largely dependent on their subcellular localization.[39] Herein, our results showed that H19 and LDHA were colocalized in the cytoplasm. Therefore, we speculated that H19 might function as a ceRNA to regulate LDHA expression by sponging miRNAs. Subsequently, there was a negative correlation between miR-519d-3p and H19 or LDHA in GC cells. Importantly, miR-519d-3p functioned as a tumor suppressor in multiple malignant tumors, such as colorectal cancer,[40] breast cancer,[41] pancreatic ductal adenocarcinoma,[42] and GC.[43]

Herein, in vitro luciferase assays indicated that both H19 and LDHA were direct targets of miR-519d-3p. Moreover, miR-519d-3p knockdown abolished the effect of H19 suppression on LDHA expression, glucose consumption, lactate production, and cell proliferation in GC. The above results revealed that H19 regulated glycolysis and cell proliferation through the miR-519d-3p/LDHA axis.

As a major glycolytic metabolite, lactate functioned as a modulator of immune response and tumor progression.[24,25,31] Lactate dehydrogenase A-associated lactate accumulation blunted tumor surveillance by inhibiting the function and survival of T and NK cells.[25] Chen et al reported that lactate could activate macrophage G protein-coupled receptor 132 (Gpr132) to promote the alternatively activated macrophage (M2)-like phenotype.[44] Furthermore, lactate was markedly upregulated in GC tumor-infiltrating T cells and associated with decreased T helper 1 cells and CTLs.[45] Based on our data that H19 affected lactate accumulation, we concluded that H19 might modulate tumor immune response in a lactate-dependent manner. Our and others' studies showed that γδT cells have important roles in tumor immunosurveillance against multiple malignancies,
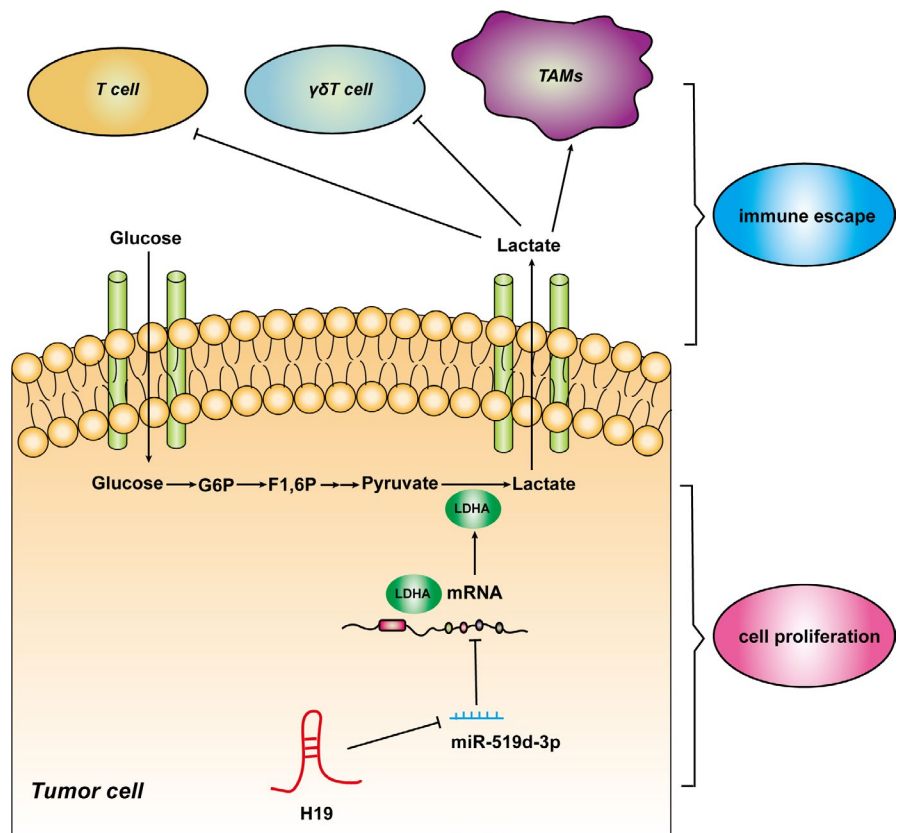
FIGURE 8 H19 modulated the aerobic glycolysis, proliferation, and immune escape of gastric cancer cells by sponging microRNA (miR)-519d-3p to induce the expression of lactate dehydrogenase A (LDHA). TAM, tumor-associated macrophage

such as colorectal cancer and leukemia.[26,46] Importantly, tumor-infiltrating γδT cells were an independent prognostic factor in GC patients and could predict the survival benefit of adjuvant chemotherapy in patients with TNM II and III diseases.[47] Therefore, we explored the effect of CM from stable knockdown H19 GC cells on γδT cells. Our results indicated that CM from stable knockdown H19 GC cells elevated the population of IFN-γ$^+$ γδT cells, while lactate or treatment with CM from stable knockdown H19 GC cells after transfection with miR-519d-3p inhibitor or LDHA overexpression plasmid counteracted this effect. In addition, we also asked how H19 knockdown affected T cells and TAMs. The addition of lactate or treatment with CM from stable knockdown H19 GC cells after transfection with miR-519d-3p inhibitor or LDHA overexpression plasmid abolished the increase in IL-2 expression in activated Jurkat cells and TAM generation induced by CM from stable knockdown H19 GC cells. These data indicated that H19 signaling could modulate the activity of γδT cells, T cells, and TAMs. Nevertheless, the effect of the H19/miR-519d-3p/LDHA/lactate axis on other immune cells, such as NK cells, myeloid-derived suppressor cells, and Foxp3 regulatory T cells, requires investigation in our future study.

In summary, our results indicated the novel role of H19 in modulating aerobic glycolysis, proliferation, and immune escape of GC. Moreover, H19 mediated the effect on aerobic glycolysis, proliferation, and immune escape of GC cells through the miR-519d-3p/LDHA axis.

ACKNOWLEDGMENTS

DISCLOSURE

The authors declare that they have no conflict of interest.

ORCID

Tongguo Shi https://orcid.org/0000-0002-5382-2775

REFERENCES

1. Bray F, Ferlay J, Soerjomataram I, Siegel R, Torre L, Jemal A. Global cancer statistics 2018: GLOBOCAN estimates of incidence and mortality worldwide for 36 cancers in 185 countries. *CA Cancer J Clin.* 2018;68:394-424.
2. Sexton R, Al Hallak M, Diab M, Azmi A. Gastric cancer: a comprehensive review of current and future treatment strategies. *Cancer Metast Rev.* 2020;39(4):1179-1203.
3. Begolli R, Sideris N, Giakountis A. LncRNAs as chromatin regulators in cancer: from molecular function to clinical potential. *Cancers.* 2019;11:1524.
4. Zhang H, Zhu C, He Z, Chen S, Li L, Sun C. LncRNA PSMB8-AS1 contributes to pancreatic cancer progression via modulating miR-382-3p/STAT1/PD-L1 axis. *J Exp Clin Cancer Res.* 2020;39:179.
5. Fang Z, Wang Y, Wang Z, et al. ERINA is an estrogen-responsive lncRNA that drives breast cancer through the E2F1/RB1 pathway. *Can Res.* 2020;80:4399-4413.
6. Gandhi M, Groß M, Holler J, et al. The lncRNA lincNMR regulates nucleotide metabolism via a YBX1 - RRM2 axis in cancer. *Nat Commun.* 2020;11:3214.
7. Zhang M, Wang N, Song P, et al. LncRNA GATA3-AS1 facilitates tumour progression and immune escape in triple-negative breast cancer through destabilization of GATA3 but stabilization of PD-L1. *Cell Prolif.* 2020;53:e12855.
8. Wang J, Xie S, Yang J, et al. The long noncoding RNA H19 promotes tamoxifen resistance in breast cancer via autophagy. *J Hematol Oncol.* 2019;12:81.
9. Zhang Y, Huang W, Yuan Y, et al. Long non-coding RNA H19 promotes colorectal cancer metastasis via binding to hnRNPA2B1. *J Exp Clin Cancer Res.* 2020;39:141.
10. Yoshimura H, Matsuda Y, Yamamoto M, et al. Reduced expression of the H19 long non-coding RNA inhibits pancreatic cancer metastasis. *Lab Invest.* 2018;98:814-824.
11. Yan J, Zhang Y, She Q, et al. Long noncoding RNA H19/miR-675 axis promotes gastric cancer via FADD/Caspase 8/Caspase 3 signaling pathway. *Cell Physiol Biochem.* 2017;42:2364-2376.
12. Lecerf C, Le Bourhis X, Adriaenssens E. The long non-coding RNA H19: an active player with multiple facets to sustain the hallmarks of cancer. *Cell Mol Life Sci.* 2019;76:4673-4687.
13. Zhang E, Han L, Yin D, Kong R, De W, Chen J. c-Myc-induced, long, noncoding H19 affects cell proliferation and predicts a poor prognosis in patients with gastric cancer. *Med Oncol.* 2014;31:914.
14. Zhou X, Ye F, Yin C, Zhuang Y, Yue G, Zhang G. The interaction between MiR-141 and lncRNA-H19 in regulating cell proliferation and migration in gastric cancer. *Cell Physiol Biochem.* 2015;36:1440-1452.
15. Li P, Tong L, Song Y, et al. Long noncoding RNA H19 participates in metformin-mediated inhibition of gastric cancer cell invasion. *J Cell Physiol.* 2019;234:4515-4527.
16. Logotheti S, Marquardt S, Gupta S, et al. LncRNA-SLC16A1-AS1 induces metabolic reprogramming during Bladder Cancer progression as target and co-activator of E2F1. *Theranostics.* 2020;10:9620-9643.
17. Ma X, Li B, Liu J, Fu Y, Luo Y. Phosphoglycerate dehydrogenase promotes pancreatic cancer development by interacting with eIF4A1 and eIF4E. *J Exp Clin Cancer Res.* 2019;38:66.
18. Fan C, Tang Y, Wang J, et al. Role of long non-coding RNAs in glucose metabolism in cancer. *Mol Cancer.* 2017;16:130.
19. Liu J, Liu Z, Wu Q, et al. Long noncoding RNA AGPG regulates PFKFB3-mediated tumor glycolytic reprogramming. *Nat Commun.* 2020;11:1507.
20. Zhao Y, Liu Y, Lin L, et al. The lncRNA MACC1-AS1 promotes gastric cancer cell metabolic plasticity via AMPK/Lin28 mediated mRNA stability of MACC1. *Mol Cancer.* 2018;17:69.
21. Peng F, Wang J, Fan W, et al. Glycolysis gatekeeper PDK1 reprograms breast cancer stem cells under hypoxia. *Oncogene.* 2018;37:1062-1074.
22. Hesketh R, Wang J, Wright A, et al. Magnetic resonance imaging is more sensitive than PET for detecting treatment-induced cell death-dependent changes in glycolysis. *Can Res.* 2019;79:3557-3569.
23. Gottfried E, Kreutz M, Mackensen A. Tumor metabolism as modulator of immune response and tumor progression. *Semin Cancer Biol.* 2012;22:335-341.
24. Ippolito L, Morandi A, Giannoni E, Chiarugi P. Lactate: a metabolic driver in the tumour landscape. *Trends Biochem Sci.* 2019;44:153-166.
25. Brand A, Singer K, Koehl G, et al. LDHA-associated lactic acid production blunts tumor immunosurveillance by T and NK cells. *Cell Metab.* 2016;24:657-671.
26. Lu H, Shi T, Wang M, et al. B7–H3 inhibits the IFN-γ-dependent cytotoxicity of Vγ9Vδ2 T cells against colon cancer cells. *Oncoimmunology.* 2020;9:1748991.
27. Zheng X, Zhou Y, Chen W, et al. Ginsenoside 20(S)-Rg3 prevents PKM2-targeting miR-324-5p from H19 sponging to antagonize the Warburg effect in ovarian cancer cells. *Cell Physiol Biochem.* 2018;51:1340-1353.

28. Wu Z, Yan L, Liu Y, et al. Inhibition of mTORC1 by lncRNA H19 via disrupting 4E-BP1/Raptor interaction in pituitary tumours. *Nat Commun*. 2018;9:4624.

29. Wang S, Ma F, Tang Z, et al. Long non-coding RNA H19 regulates FOXM1 expression by competitively binding endogenous miR-342-3p in gallbladder cancer. *J Exp Clin Cancer Res*. 2016;35:160.

30. Vennin C, Spruyt N, Robin Y, Chassat T, Le Bourhis X, Adriaenssens E. The long non-coding RNA 91H increases aggressive phenotype of breast cancer cells and up-regulates H19/IGF2 expression through epigenetic modifications. *Cancer Lett*. 2017;385:198-206.

31. Husain Z, Huang Y, Seth P, Sukhatme V. Tumor-derived lactate modifies antitumor immune response: effect on myeloid-derived suppressor cells and NK cells. *J Immunol*. 1950;2013(191):1486-1495.

32. Thelen F, Witherden D. Get in touch with dendritic epithelial T cells!. *Front Immunol*. 2020;11:1656.

33. Gan L, Lv L, Liao S. Long non-coding RNA H19 regulates cell growth and metastasis via the miR-22-3p/Snail1 axis in gastric cancer. *Int J Oncol*. 2019;54:2157-2168.

34. Liu G, Xiang T, Wu Q, Wang W. Long noncoding RNA H19-derived miR-675 enhances proliferation and invasion via RUNX1 in gastric cancer cells. *Oncol Res*. 2016;23:99-107.

35. Li X, Zhang C, Zhao T, et al. Lysine-222 succinylation reduces lysosomal degradation of lactate dehydrogenase a and is increased in gastric cancer. *J Exp Clin Cancer Res*. 2020;39:172.

36. Zhu W, Ma L, Qian J, et al. The molecular mechanism and clinical significance of LDHA in HER2-mediated progression of gastric cancer. *Am J Transl Res*. 2018;10:2055-2067.

37. Wang H, Zhou R, Sun L, et al. TOP1MT deficiency promotes GC invasion and migration via the enhancements of LDHA expression and aerobic glycolysis. *Endocr Relat Cancer*. 2017;24:565-578.

38. Wei C, Gao J. Downregulated miR-383-5p contributes to the proliferation and migration of gastric cancer cells and is associated with poor prognosis. *PeerJ*. 2019;7:e7882.

39. Liang Y, Song X, Li Y, et al. LncRNA BCRT1 promotes breast cancer progression by targeting miR-1303/PTBP3 axis. *Mol Cancer*. 2020;19:85.

40. Tang X, Sun G, He Q, et al. Circular noncoding RNA circMBOAT2 is a novel tumor marker and regulates proliferation/migration by sponging miR-519d-3p in colorectal cancer. *Cell Death Dis*. 2020;11:625.

41. Li D, Song H, Wu T, et al. MiR-519d-3p suppresses breast cancer cell growth and motility via targeting LIM domain kinase 1. *Mol Cell Biochem*. 2018;444:169-178.

42. Sun J, Zhang P, Yin T, Zhang F, Wang W. Upregulation of LncRNA PVT1 facilitates pancreatic ductal adenocarcinoma cell progression and glycolysis by regulating MiR-519d-3p and HIF-1A. *J Cancer*. 2020;11:2572-2579.

43. Li Y, Shao J, Zhang S, Xing G, Liu H. miR-519d-3p inhibits cell proliferation and invasion of gastric cancer by downregulating B-cell lymphoma 6. *Cytogenet Genome Res*. 2018;154:12-19.

44. Chen P, Zuo H, Xiong H, et al. Gpr132 sensing of lactate mediates tumor-macrophage interplay to promote breast cancer metastasis. *Proc Natl Acad Sci USA*. 2017;114:580-585.

45. Ping W, Senyan H, Li G, Yan C, Long L. Increased lactate in gastric cancer tumor-infiltrating lymphocytes is related to impaired T cell function due to miR-34a deregulated lactate dehydrogenase A. *Cell Physiol Biochem*. 2018;49:828-836.

46. Benyamine A, Le Roy A, Mamessier E, et al. BTN3A molecules considerably improve Vγ9Vδ2T cells-based immunotherapy in acute myeloid leukemia. *Oncoimmunology*. 2016;5:e1146843.

47. Wang J, Lin C, Li H, et al. Tumor-infiltrating γδT cells predict prognosis and adjuvant chemotherapeutic benefit in patients with gastric cancer. *Oncoimmunology*. 2017;6:e1353858.

SUPPORTING INFORMATION

Additional supporting information may be found online in the Supporting Information section.